Supporting Information

Interfacing an ion mobility spectrometry based explosive trace detector to a triple quadrupole mass spectrometer

Joseph Kozole[1,2*], Jason R. Stairs[1], Inho Cho[1,2], Jason D. Harper[1,2], Stefan R. Lukow[1], Richard T. Lareau[1], Reno DeBono[3], and Frank Kuja[3]

[1]U.S. Department of Homeland Security Science &Technology Directorate
Transportation Security Laboratory
William J. Hughes Technical Center
Atlantic City International Airport, NJ 08405, USA

[2]Nova Research, Inc.
1900 Elkin Street, Suite 230, Alexandria, VA 22308, USA

[3]Smiths Detection, Inc.
7030 Century Avenue, Mississauga, Ontario, Canada

Abstract

Additional data that demonstrates the utility of the COTS-ETD/API 2000® configuration is provided. This data includes mass, mobility, and mass-selected ion mobility spectra for the explosive standards cyclo-1,3,5-trimethylene-2,4,6-trinitramine (RDX) and pentaerythritol tetranitrate (PETN). This analysis determined that the predominant product ions for RDX are $[RDX+Cl]^-$, $[RDX+NO_2]^-$, and $[RDX+RDX+Cl]^-$ and have reduced mobility values of 1.47, 1.42, and 1.00 $cm^2V^{-1}sec^{-1}$ respectively, whereas, the predominant product ions for PETN are $[NO_3]^-$, $[PETN-NO_2+H+Cl]^-$, $[PETN-H]^-$, $[PETN+Cl]^-$ and $[PETN+NO_3]^-$ and have reduced mobility values of 2.40, 1.29, 1.27, 1.22, and 1.18 $cm^2V^{-1}sec^{-1}$ respectively.

SI. Experimental

A. Sample Preparation

To prepare 100 ng samples of cyclo-1,3,5-trimethylene-2,4,6-trinitramine (RDX) and pentaerythritol tetranitrate (PETN) for analysis by the IMS/MS/MS instrument, dissolved solutions of RDX and PETN with concentrations of 100 μg/mL were deposited onto PTFE filters in 1 μL aliquots and dried under a flow of nitrogen gas.

SII. Results and Discussion

To further demonstrate the utility of the COTS-ETD/API 2000® configuration, the reduced mobility values for the ion species formed during the analysis of the explosive standards RDX and PETN were measured.

A. Mass and Mass-Selected Ion Mobility Spectra for RDX and PETN

A series of spectra resulting from the analysis of a 100 ng RDX sample is shown in figure S1. Figure S1a is the mass spectrum obtained in the continuous ion flow mode, figure S1b is the multiple mass mobility spectrum, and the plots in figure S1c are the individual mass-selected ion mobility spectra for $[Cl]^-$ at m/z 35, $[Cl_2]^-$ at m/z 70, $[RDX+Cl]^-$ at m/z 257, $[RDX+NO_2]^-$ at m/z 268, and $[RDX+RDX+Cl]^-$ at m/z 479. All peak assignments were verified using tandem MS. The spectra indicate that the predominant product ions for RDX are $[RDX+Cl]^-$, $[RDX+NO_2]^-$, and $[RDX+RDX+Cl]^-$ and have reduced mobility values of 1.47, 1.42, and 1.00 $cm^2V^{-1}sec^{-1}$ respectively.

A series of spectra resulting from the analysis of a 100 ng PETN sample is shown in figure S2. Figure S2a is the mass spectrum obtained in the continuous ion flow mode, figure S2b is the multiple mass mobility spectrum, and the plots in figure S2c are the individual mass-selected ion mobility spectra for $[Cl]^-$ at m/z 35, $[NO_3]^-$ at m/z 62, $[Cl_2]^-$ at m/z 70, $[PETN-NO_2+H+Cl]^-$ at m/z 306, $[PETN-H]^-$ at m/z 315, $[PETN+Cl]^-$ at m/z 351, and $[PETN+NO_3]^-$ at 378. All peak assignments were verified using tandem MS. The spectra indicate that the predominant product ions for PETN are $[NO_3]^-$, $[PETN-NO_2+H+Cl]^-$, $[PETN-H]^-$, $[PETN+Cl]^-$ and $[PETN+NO_3]^-$ and have reduced mobility values of 2.40, 1.29, 1.27, 1.22, and 1.18 $cm^2V^{-1}sec^{-1}$ respectively.

The mass and mass-selected in mobility spectra shown in figure S1 and figure S2 indicate that the predominant product ions for RDX and PETN are formed via ion-molecule attachment reactions with either Cl^- from the reagent chemical or NO_x^- from the decomposition of the parent molecules (i.e. autoionization), findings that are consistent with the ionization processes previously reported[1-4]. Moreover, the reduced mobility values measured using the IMS/MS/MS instrument for the product ions for RDX and PETN are consistent with the values previously reported[1-4]. Collectively, these findings provide additional evidence that the COTS-ETD/API 2000® configuration is useful for the accurate and extensive characterization of the gas phase ion chemistry of the COTS-ETD equipment

References

(1) Ewing, R. G.; Atkinson, D. A.; Eiceman, G. A.; Ewing, G. J. *Talanta* 2001, *54*, 515.
(2) Danylewych-May, L. L. *Proc. 1st Int. Sym. Explosive Detection Technology* 1991, *Atlantic City, NJ*, 672.
(3) Fetterolf, D. D.; Clark, T. D. *J. Forensic Sci.* 1993, *38*, 28.
(4) Asbury, G. R.; Klasmeier, J.; Jr., H. H. H. *Talanta* 2000, *50*, 1291.

Figure Captions

Figure S1: (a) Mass, (b) multiple mass mobility, and (c) mass-selected ion mobility spectra resulting from the analysis of a 100 ng RDX sample. The mass-selected ion mobility spectra are for $[Cl]^-$ at m/z 35 (brown), $[Cl_2]^-$ at m/z 70 (red), $[RDX+Cl]^-$ at m/z 257 (black), $[RDX+NO_2]^-$ at m/z 268 (green), and $[RDX+RDX+Cl]^-$ at m/z 479 (blue).

Figure S2: (a) Mass, (b) multiple mass mobility, and (c) mass-selected ion mobility spectra resulting from the analysis of a 100 ng PETN sample. The mass-selected ion mobility spectra are for $[Cl]^-$ at m/z 35 (grey), $[NO_3]^-$ at m/z 62 (brown), $[Cl_2]^-$ at m/z 70 (red), $[PETN-NO_2+H+Cl]^-$ at m/z 306 (gold), $[PETN-H]^-$ at m/z 315 (green), $[PETN+Cl]^-$ at m/z 351 (blue), and $[PETN+NO_3]^-$ at m/z 378 (black).

Figures

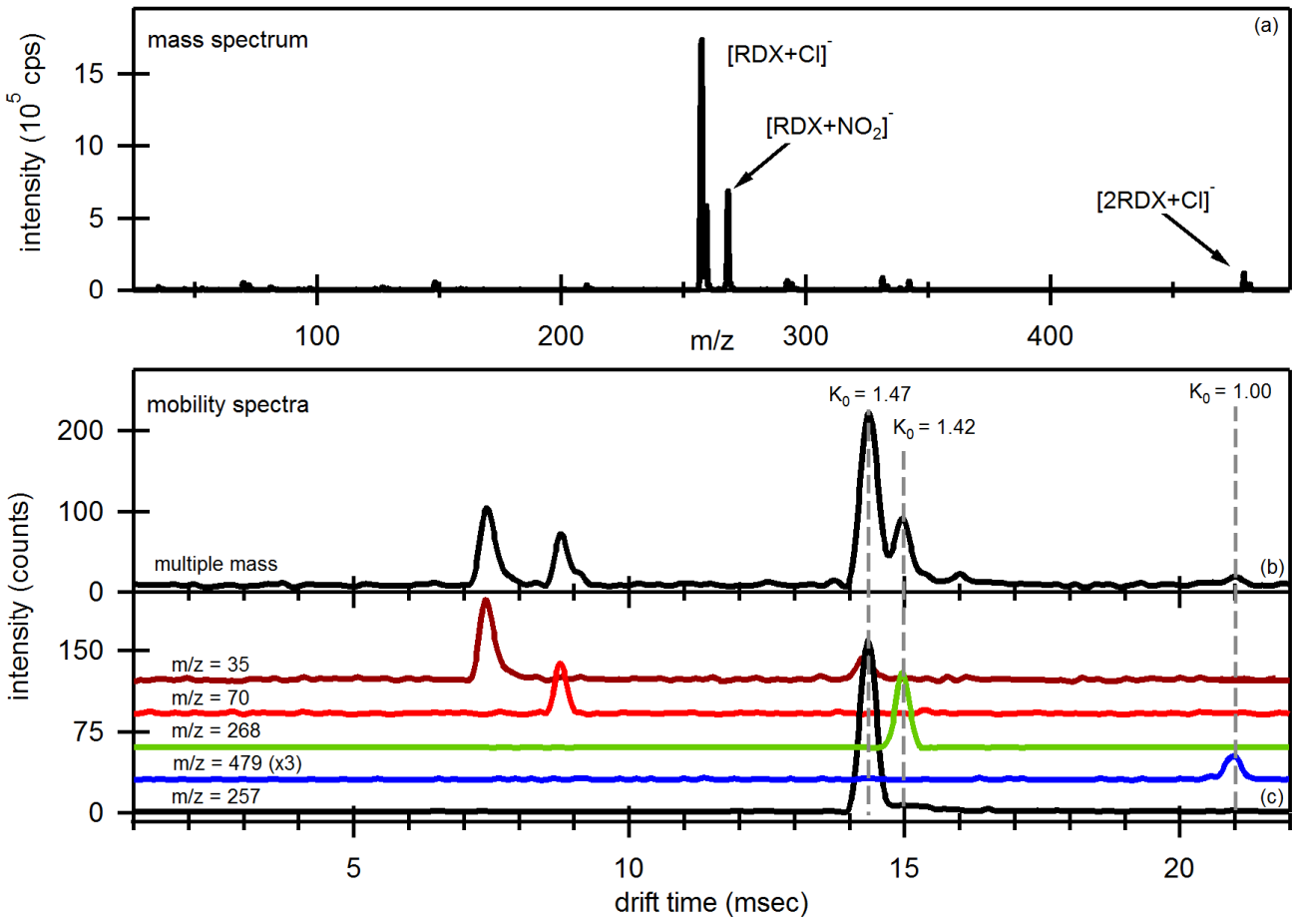
mass spectrum
(a)
[RDX+Cl]-
[RDX+NO2]-
[2RDX+Cl]-
intensity (10^5 cps)
15
10
5
0
100
200
m/z
300
400
mobility spectra
K0 = 1.47
K0 = 1.42
K0 = 1.00
multiple mass
(b)
intensity (counts)
200
100
0
150
75
0
m/z = 35
m/z = 70
m/z = 268
m/z = 479 (x3)
m/z = 257
(c)
5
10
15
20
drift time (msec)

Figure S1

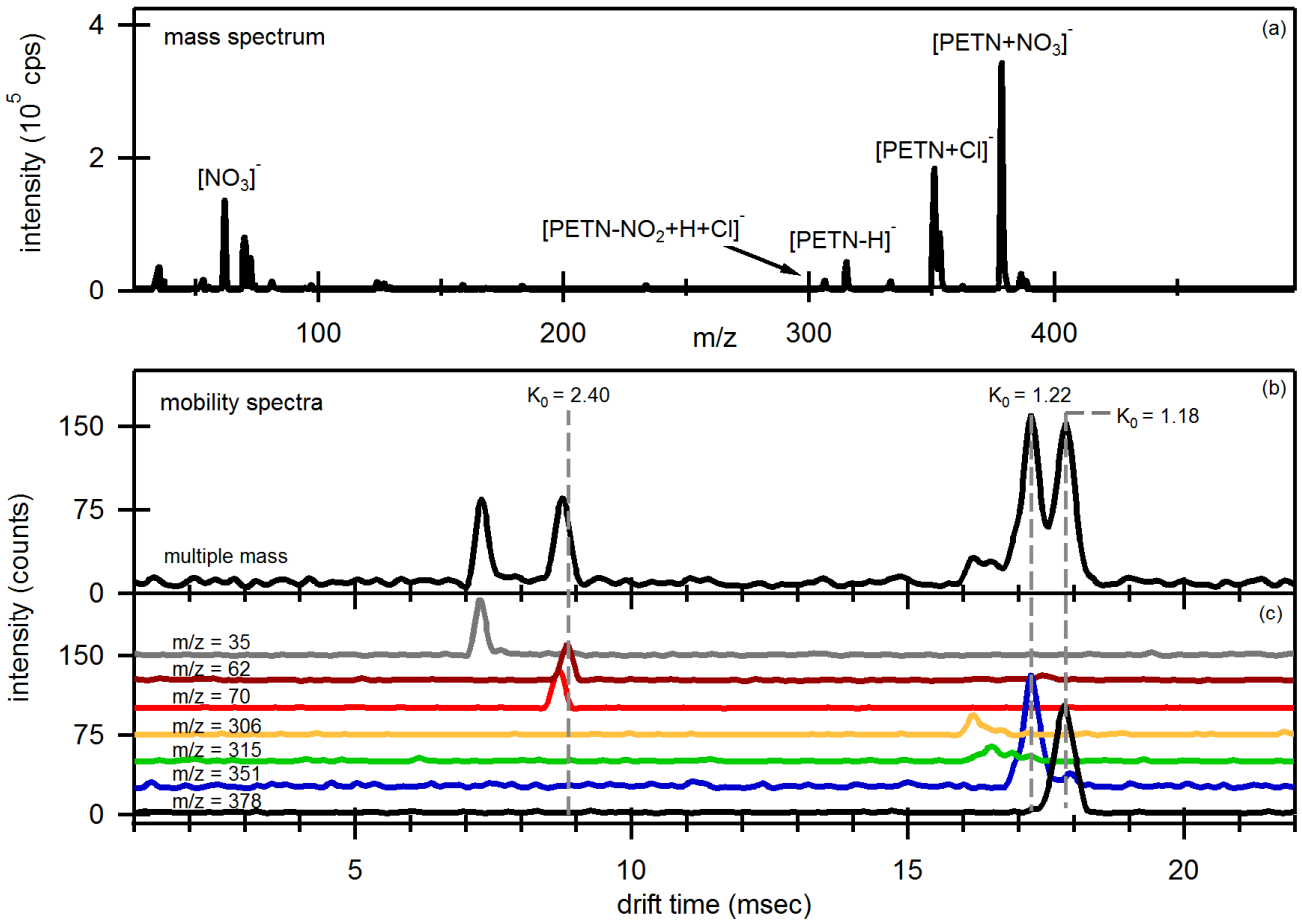
mass spectrum
(a)
intensity (10^5 cps)
4
2
0
[NO3]-
[PETN-NO2+H+Cl]-
[PETN-H]-
[PETN+Cl]-
[PETN+NO3]-
100
200
m/z
300
400
mobility spectra
(b)
K0 = 2.40
K0 = 1.22
K0 = 1.18
150
75
0
multiple mass
(c)
intensity (counts)
m/z = 35
m/z = 62
m/z = 70
m/z = 306
m/z = 315
m/z = 351
m/z = 378
150
75
0
5
10
15
20
drift time (msec)

Figure S2